PROCEEDINGS OF SCIENCE

Joint search for gravitational waves and high-energy neutrinos with the ANTARES, LIGO and Virgo detectors

V. Van Elewyck[*,a]
for the ANTARES Collaboration, the LIGO Scientific Collaboration and the Virgo Collaboration

[a]*APC, Université Paris Diderot, CNRS/IN2P3, CEA/Irfu, Obs. de Paris, Sorbonne Paris Cité, France*
E-mail: elewyck@apc.univ-paris7.fr

Cataclysmic cosmic events can be plausible sources of both gravitational waves (GW) and high-energy neutrinos (HEN), alternative cosmic messengers carrying information from the innermost regions of the astrophysical engines. Possible sources include long and short gamma-ray bursts (GRBs) but also low-luminosity or choked GRBs, with no or low gamma-ray emissions. Combining directional and timing informations on HEN events and GW bursts through GW+HEN coincidences provides a novel way of constraining the processes at play in the sources. It also enables to improve the sensitivity of both channels relying on the independence of backgrounds in each experiment. A first search was performed with concomitant data from 2007, when ANTARES was half its final size. This contribution focuses on the second, optimised search performed with data taken in 2009-2010, during the Virgo VSR2-3 and LIGO L6 science runs (with improved sensitivity) and with ANTARES in its final configuration. While the 2007 search has allowed to place the first upper limits on the density of joint GW+HEN emitters, the 2009-2010 analysis will provide a significant improvement in sensitivity.

The 34th International Cosmic Ray Conference,
30 July- 6 August, 2015
The Hague, The Netherlands

*Speaker.

PoS(ICRC2015)1112

1. Introduction

Multimessenger astronomy is at a turning point with the first cosmic High-Energy Neutrinos (HEN) detection by the IceCube experiment [1] and the very probable detection of Gravitational Waves (GW) with the advanced generation of the LIGO [2] and Virgo [3] detectors. In this context, a new window is about to open for the observation of the Universe with cosmic messengers conserving timing and directionality, complementary to electromagnetic observations. Both HEN and GW are expected to provide important information about the processes taking place in the core of astrophysical production sites. They could even reveal the existence of electromagnetically dark sources, that would have remained undetected so far, such as the putative "choked GRBs" which could constitute the missing link between core-collapse Supernovae and GRBs. A detailed discussion of potential GW+HEN emitters can be found in [4].

The first concomitant data-taking phase with the whole Virgo/LIGO network, VSR1/S5, was carried out in 2007, while ANTARES [5] was operating in a five-line configuration. The strategy chosen for the 2007 GW+HEN joint search consisted in an event-by-event search for a GW signal correlating in space and time with a given HEN event considered as an external trigger [6]. This approach allowed to make use of existing GW analysis pipelines developed e.g. for GRB searches. The list of 2007 HEN triggers was obtained by applying on ANTARES data a standard reconstruction algorithm (BBFit [7]) and quality requirements similar to those selecting the well-reconstructed events that are used for the standalone searches for HEN point sources. The list of HEN triggers included their arrival time, direction on the sky, and an event-by-event estimation of the angular accuracy, which was used to define the angular search window for the GW search.

This list was then processed by the X-pipeline [8], an algorithm which performs coherent searches for unmodelled bursts of GWs on the combined data stream coming from all interferometers. The background estimation and the optimization of the selection strategy were performed using time-shifted data from the off-source region in order to avoid contamination by a potential GW signal. Once the search parameters were tuned, the analysis was applied to the on-source dataset, consisting of data recorded within a time window of $[-500s, +500s]$ around the time of each HEN trigger. This time interval was chosen on basis of conservative estimations of the time delay between the HEN and GW signals expected for long GRBs, based on BATSE, *Swift* and *Fermi* observations [9]. No GW candidate was observed in coincidence with the selected HEN events from the 2007 data sample. A binomial test was also performed to look for an accumulation of weak GW signals, with negative results. This allowed to extract GW exclusion distances for typical source scenarios. Converting this null observation into a density of GW+HEN emitters yielded a limit ranging from 10^{-2} Mpc^{-3} yr^{-1} for short GRB-like signals down to 10^{-3} Mpc^{-3} yr^{-1} for long GRB-like emissions [6].

This contribution focuses on the second search that is being finalized with data taken with the full ANTARES detector in 2009-2010, concomitant with the Virgo VSR2/VSR3 and LIGO S6 joint science runs, with upgraded GW detectors. Building on the experience of the pioneering 2007 search, and following the joint 2009 IceCube-LIGO-Virgo analysis [10] which introduced a more complete and symmetrical characterisation of the GW and HEN events [11], a new strategy has been adopted for the optimisation of the HEN trigger list in order to maximise the number of sources detectable by the search. A new HEN reconstruction algorithm (AAfit) has been used in

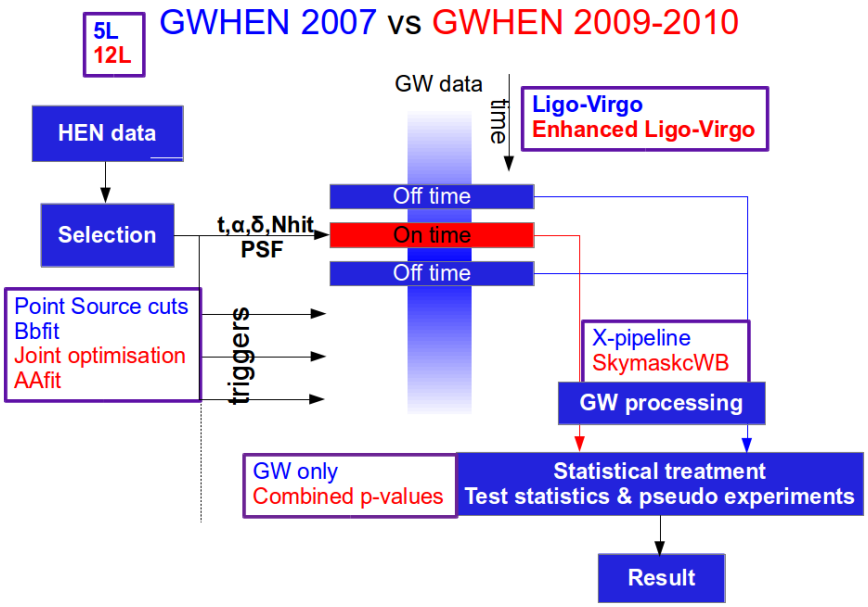

Figure 1: Schematic flow diagram of the ANTARES/Virgo/LIGO GW+HEN analysis strategies used for the 2007 and 2009-2010 joint searches. In both cases, the neutrino candidates (with their time and directional information) act as external triggers for a given GW analysis pipeline, which searches the combined GW data flow from all active interferometers (ITFs) for a possible concomitant signal. The background estimation and the optimization of the selection strategy are performed using time-shifted data from the off-source region in order to avoid contamination by a potential GW signal. Once the search parameters are tuned, the box is opened and the analysis is applied to the on-source dataset.

order to reduce the angular error [12]. A different GW pipeline, the skymask coherent WaveBurst (s-cWB), has also been developed to allow the analysis with only 2 interferometers taking data, and the realisation of joint simulations - a necessary step to optimise the joint analysis [13]. Figure 1 presents a flowchart of the analysis highlighting the main differences and improvements between the 2007 and the 2009-2010 joint searches.

Section 2 describes the detector configuration and datasets used for the 2009-2010 joint search, and Section 3 presents the strategy and statistical tools used for the joint optimisation procedure. Perspectives on the expected sensitivity of the search are discussed in Section 4.

2. Detectors and associated datasets

2.1 The ANTARES neutrino telescope and associated dataset

The ANTARES telescope [5] is located at a depth of 2475m in the Mediterranean Sea off the coast of Toulon, at $42°48' N, 6°10' E$. It comprises 885 optical modules consisting in 17" glass spheres, each of them housing one 10" photomultiplier, and installed on 12 vertical strings.

The dataset used in this analysis covers the period from July 7th 2009 to October 20th 2010 for a total observation time of 266 days. The sample consists in events originating from muon neutrino charged-current interactions, which produce a muon that leaves a track-like signal in the detector. It is the most suited to this kind of directional searches, as the current reconstruction algorithms for this class of events achieve a sub-degree angular resolution (defined as the median

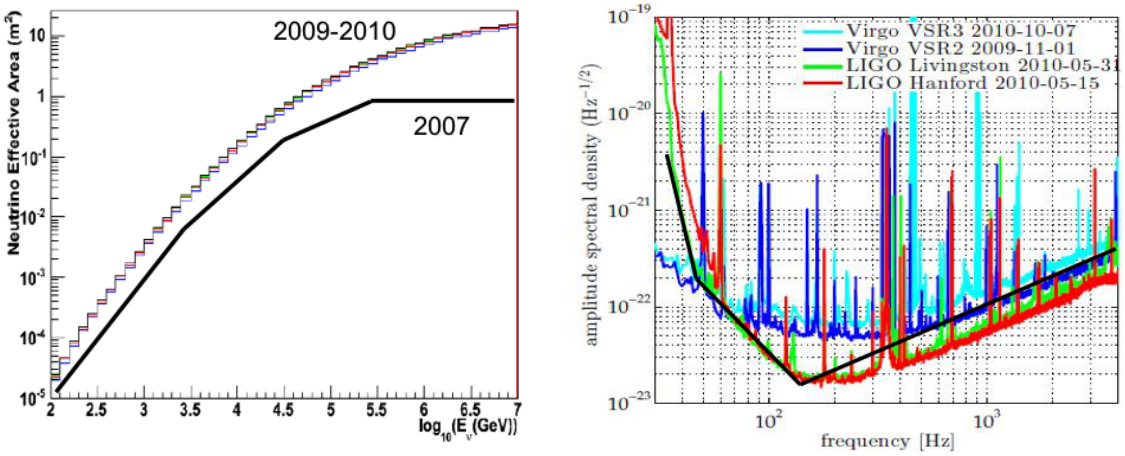

Figure 2: Left: ANTARES effective area A_{eff} for the two detector configurations corresponding to the datasets used in GW+HEN searches: 2007 and 2009-2010 (where the colors correspond to different sets of quality cuts on the event reconstruction). **Right:** Detector noise spectra for LIGO and Virgo, showing typical sensitivities for the S6-VSR2/3 datasets (2009-2010). Also shown in black, to guide the eye, is the sensitivity representative of the first LIGO science run, S5 (2007).

angle between the neutrino and the reconstructed muon). The effective area A_{eff} of the detector is plotted against energy in Figure 2 (left). It represents the detector response function as a function of the neutrino energy, and yields the detection rate for a given neutrino flux. The figure shows a clear increase between the 2007 datasample (5-line detector) used for the first GW+HEN search, and the 2009-2010 datasample (full, 12-line detector) used for this analysis.

2.2 The LIGO and Virgo gravitational wave interferometers and associated data set

LIGO [2], with two sites in the United States, and Virgo [3], with one site in Italy, consist of perpendicular km-size Fabry-Perot cavities forming a Michelson interferometer tuned to the dark fringe. Any gravitational wave passing through the detector would induce a difference of path length in the two arms, thus changing the interference pattern. The direction of an event is reconstructed by time-of-flight techniques which imply the use of at least two detectors. Figure 2 (right) shows the typical sensitivity for the LIGO and Virgo science runs taken in 2009 and 2010, compared to the one achieved in 2007.

The GW data used in this search are the S6-VSR2/3 LIGO-Virgo data, which were collected between July 07, 2009 and October 21, 2010 by three detectors: LIGO-Livingston, LIGO-Hanford and Virgo. The concomitant data taking period between S6-VSR2/3 and ANTARES comprises all periods during which at least two out of the three interferometers were in science mode; the total duration of the joint dataset used for this analysis is $\tau \equiv$128.7 days.

3. Joint optimisation of the common dataset

3.1 Definition of the joint figure of merit

The approach adopted here is to optimise the HEN and GW selection cuts in order to maxi-

mize the number $\mathcal{N}_{\mathrm{GWHEN}}$ of detectable sources emitting both GW and HEN. A trade-off should therefore be found between two competing trends. Relaxing the cuts on the HEN sample will enhance efficiency to HEN signal, thereby increasing the number of suitable candidates; but this will require harder cuts on the GW candidate sample in order to maintain the False Alarm Rate (FAR) below a fixed value.

Let us assume here that the sources are all identical and radiate an energy E_{GW} in GW and emit a fluence φ_ν in HEN, and that their population is isotropic, i.e. characterised by a constant density per unit time and volume, R. The number of detectable sources is then given by

$$\mathcal{N}_{\mathrm{GWHEN}}(\mathrm{cuts}) = \int dt d^3\Omega \mathscr{R}(r,t)\varepsilon_\nu(\mathrm{cuts})\varepsilon_{GW}(\mathrm{cuts};E_{GW},r) \tag{3.1}$$

where $\mathscr{R}(r,t) = R\,\mathscr{P}(N_\nu > 0|\frac{\varphi_\nu}{4\pi r^2})$ is the density of detectable sources. From Poisson statistics, we get $\mathscr{P}(N_\nu > 0|\frac{\varphi_\nu}{4\pi r^2}) \propto \frac{1}{r^2}$ in the limit of small fluxes. The optimisation is performed by varying the cut thresholds applied to the two following parameters: the quality of the muon track reconstruction Λ for the HEN event sample, and a proxy to the signal-to-noise ratio ρ for the GW event sample, respectively. We obtain

$$\mathcal{N}_{\mathrm{GWHEN}}(\Lambda,\rho_{threshold}) \propto \int_0^\infty 4\pi r^2 dr\,\frac{1}{r^2}\varepsilon_\nu(\Lambda)\varepsilon_{GW}(\rho_{threshold};E_{GW},r) \tag{3.2}$$

where ε_{GW} and ε_{HEN} are the respective detector efficiencies to signal. ε_{GW} can be reasonably well approximated by a step-like function with the edge placed at the maximum distance $D(\rho_{threshold})$ at which a GW source is detectable, defined as the GW *horizon*; therefore,

$$\mathcal{N}_{\mathrm{GWHEN}}(\Lambda,\rho_{threshold}) \propto \varepsilon_\nu(\Lambda)\int_0^{D(\rho_{threshold})} dr \tag{3.3}$$

For a GW "standard candle", $\rho_{threshold}$ is inversely proportional to $D(\rho_{threshold})$, leading to

$$\mathcal{N}_{\mathrm{GWHEN}}(\Lambda,\rho_{threshold}) \propto \varepsilon_\nu(\Lambda)/\rho_{threshold} \tag{3.4}$$

The procedure then consists in tuning the HEN selection cuts in order to maximise the GWHEN figure of merit given by the ratio $\varepsilon_\nu(\Lambda)/\rho_{threshold}$. As can be seen from Figure 3 (left), the optimal cut leads to 1986 neutrino candidates, each of them characterized by its arrival time, sky direction, energy and associated error box. The energy estimator is the number of hits (or n^{hit}) used in the track fit. The error box, which depends on the track energy, is defined as the 90% percentile of the distribution of space angles ψ between the reconstructed muon and the incident neutrino direction, as estimated from Monte Carlo simulations. To each neutrino candidate i is associated a p-value p_i^{HEN} representing the probability that the atmospheric neutrino background would produce an event with at least the same number of hits as the considered event. Figure 3 (right) displays the skymap of the selected events, together with their error box, or angular search window (ASW90%) used for the subsequent GW search.

For each of the selected neutrino events, the adapted pipeline skymask coherent WaveBurst (s-cWB) [13] performs a search for GW around the neutrino time. Among the 1986 candidate HEN, 773 are associated with 2 or more GW interferometers taking data, and are therefore usable for the purposes of the joint search. The whole sky is not scanned but only the region corresponding

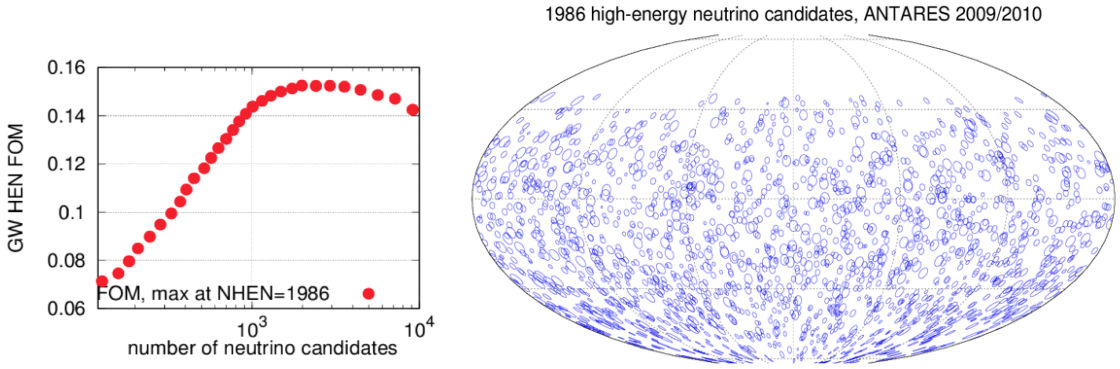

Figure 3: Left: Joint GW-HEN figure of merit as a function of the number of selected HEN candidates (as determined by the value of the threshold cut on Λ). **Right:** Skymap of the 1986 selected HEN events with their associated ASW90% angular error box.

to ASW90% centered on the reconstructed arrival direction of the neutrino $\vec{\mathbf{d}}_0$. For each candidate, s-cWB provides the GW skymap labeled hereafter $\mathscr{F}_i^{\mathrm{GW}}(\vec{\mathbf{d}})$ within ASW90%. These "sky-maps" are made of pixels of $0.4^\circ \times 0.4^\circ$, each associated with the probability that a GW is coming from it. The reconstruction pipeline also provides the value of ρ for each GW candidates. This latter will correspond to a false alarm rate $\mathrm{FAR_i}(\rho_i)$ which in turn can be associated to a GW p-value indicating the probability that coherently combined background from different GW interferometers produces an event with at least this value of ρ_i, defined as:

$$p_i^{\mathrm{GW}} = 1 - P(0|\tau_i \times \mathrm{FAR_i}(\rho_i)) \tag{3.5}$$

where τ_i is the duration of the GW interferometers run in a certain configuration (*i.e.* combination of active detectors) during which event i was recorded. The distributions are computed using $O(10^3)$ background realisations obtained with time shifts of the data stream.

3.2 Statistical characterisation of the joint candidates

The direction of the joint candidate event can be defined as the one maximizing the convolution of the GW skymaps and HEN point-spread functions (PSFs) $\mathscr{F}_i^{\mathrm{GW}}$ and $\mathscr{F}_i^{\mathrm{HEN}}$.

The joint directional test statistic relies on the marginalized likelihood of the joint event, defined as:

$$\ln(\mathscr{L}_i) = \ln\left(\int \mathscr{F}_i^{\mathrm{GW}}(\vec{x}) \times \mathscr{F}_i^{\mathrm{HEN}}(\vec{x}) d\vec{x}\right) \tag{3.6}$$

and the p-value corresponding to the combined PSF-likelihood is given by:

$$p_i^{sky} = \int_{\mathscr{L}_i}^{\infty} P_{bg}(\ln(\mathscr{L}))d\mathscr{L} \tag{3.7}$$

3.3 Final test statistic

The three obtained p-values can be combined using Fisher's method [14] to construct a test statistic for each event i:

$$X_i^2 = -2\ln(p_i^{sky} \times p_i^{\mathrm{GW}} \times p_i^{\mathrm{HEN}}) \tag{3.8}$$

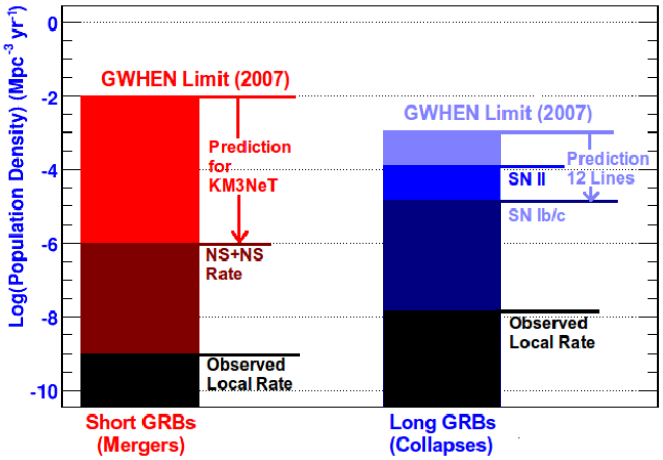

Figure 4: GWHEN 2007 astrophysical limits as compared with local short/long GRB rates, merger rates, and SN II and SN Ib/c rates. Also shown is the expected reach of ongoing (2009-2010) and future analyses.

The final result of the search is the p-value of its most significant event i defined as:

$$p^{\mathrm{GWHEN}} = \int_{Max(X_i^2)}^{\infty} P_{bg}(max(X^2))dX^2 \tag{3.9}$$

The background probability density function $P_{bg}(max(X^2))$ is estimated by a Monte Carlo simulation of 10^4 pseudo-experiments of 773 joint triggers (the remaining of the 1986 neutrinos coincident with data taking periods of GW interferometers) obtained by applying the analysis on time-shifted GW data. It will determine the significance of the loudest event once the box will be opened and the real, non-time-shifted data will be scrutinized. An accumulation of weaker signals can also be looked for, as was performed for the 2007 joint search.

4. Perspectives and expected sensitivity

The pioneering GW+HEN searches developed in [6] and [10] have opened the way towards a new multimessenger astronomy. Beyond the benefits of a potential high-confidence discovery, future analyses could be able to constrain the density of joint sources down to astrophysically meaningful levels. Figure 4 shows the upper limits on the population density of common HEN and GW emitters obtained from the ANTARES/Virgo/LIGO 2007 joint search, together with the potential reach of the ongoing (and future) searches.

The previous discussion and the flow diagram of Figure 1 help understand the sources of the global improvement expected on these limits. The equivalent live time of the analysis is increased by 40% with respect to the 2007 search, a gain which is also related to the possibility offered by the s-CWB pipeline to exploit data with only two interferometers active. The effective area of ANTARES has been multiplied by ~ 3 above 100 TeV during this data taking period. Combined with the enhanced sensitivity of the GW interferometers, and with the improvements in reconstruction and optimisation algorithms, a net gain by a factor ~ 8 can be expected with respect to what was achieved in the 2007 search.

This new search should for example allow to constrain the population of events of core-collapse type at the order of 10^{-4} $\mathrm{Mpc}^{-3}\mathrm{yr}^{-1}$ which is the observed rate of core-collapse supernovae. It also opens the path for the future with the advanced version of GW interferometers aLigo and aVirgo which will have ten-fold sensitivity [15] and will be operated at the same time as kilometric-scale neutrino detectors IceCube and KM3NeT [16].

References

[1] M. G. Aartsen *et al.* [IceCube Collaboration], *Evidence for High-Energy Extraterrestrial Neutrinos at the IceCube Detector,* Science **342** (2013) 1242856 [arXiv:1311.5238].

[2] B. P. Abbott *et al.* [LIGO Scientific Collaboration], *LIGO: The Laser interferometer gravitational-wave observatory,* Rept. Prog. Phys. **72** (2009) 076901 [arXiv:0711.3041].

[3] T. Accadia et al., *Status of the Virgo project,* Class. Quant. Grav. **28** (2011) 114002.

[4] S. Ando et al., *Colloquium: Multimessenger astronomy with gravitational waves and high-energy neutrinos,* Rev. Mod. Phys. **85** (2013) 4, 1401 [arXiv:1203.5192].

[5] M. Ageron et al. , *Nucl. Instrum. Methods* A **656**, 11 (2011)

[6] The ANTARES collaboration, the Ligo Collaboration and the Virgo Collaboration, *A First Search for coincident Gravitational Waves and High-Energy Neutrinos using LIGO, Virgo and ANTARES data from 2007,* JCAP **1306** (2013) 008 [arXiv:1205.3018].

[7] J. A. Aguilar et al. [ANTARES Collaboration], *A fast algorithm for muon track reconstruction and its application to the ANTARES neutrino telescope*, Astropart. Phys. 34 (2011) 652-662, [arXiv:1105.4116].

[8] P. J. Sutton et al., *X-Pipeline: An Analysis package for autonomous gravitational-wave burst searches*, New J. Phys. **12** (2010) 053034 [arXiv:0908.3665 [gr-qc]].

[9] B. Baret *et al., Bounding the Time Delay between High-energy Neutrinos and Gravitational-wave Transients from Gamma-ray Bursts,'* Astropart. Phys. **35** (2011) 1 [arXiv:1101.4669].

[10] The IceCube Collaboration, the Ligo Collaboration and the Virgo Collaboration *Phys. Rev.* D **90**, 102002 (2014)

[11] B. Baret et al., *Multimessenger Science Reach and Analysis Method for Common Sources of Gravitational Waves and High-energy Neutrinos,* Phys. Rev. D **85** (2012) 103004 [arXiv:1112.1140].

[12] S. Adrian-Martinez *et al.* [Antares Collaboration], *First Search for Point Sources of High-Energy Cosmic Neutrinos with the ANTARES Neutrino Telescope,* Astrophys. J. **743** (2011) L14 [arXiv:1108.0292].

[13] B. Bouhou, PhD of Université P. et M. Curie Paris VI (2012), https://tel.archives-ouvertes.fr/tel-00819985

[14] R. A. FISHER, *Statistical Methods for Research Workers*, Oliver and Boyd (Edinburgh), (1925).

[15] G. M. Harry [LIGO Scientific Collaboration], *Advanced LIGO: The next generation of gravitational wave detectors,* Class. Quant. Grav. **27** (2010) 084006.

[16] KM3NeT Technical Design Report, ISBN-978-90-6488-033-9.